PNAS
www.pnas.org

Supplementary Information for

The role of critical micellization concentration in efficacy and toxicity of supramolecular polymers

Hao Su, Feihu Wang, Wei Ran, Weijie Zhang, Wenbing Dai, Han Wang, Caleb F. Anderson, Zongyuan Wang, Chao Zheng, Pengcheng Zhang, Yaping Li and Honggang Cui*

Honggang Cui
Email: hcui6@jhu.edu

This PDF file includes:

Supplementary text
Figs. S1 to S17
Tables S1
References for SI reference citations

www.pnas.org/cgi/doi/10.1073/pnas.1913655117

Supplementary Information Text

Chemicals. Resin and Fmoc amino acids (Fmoc-Lys(Fmoc)-OH) were purchased from Advanced Automated Peptide Protein Technologies (AAPPTEC, Louisville, KY, USA). Fmoc-Lys(Fmoc)-OH was purchased from Novabiochem (San Diego, CA, USA). $mPEG_4$-CH_2CH_2COOH (OEG_5-COOH) was purchased from PurePEG LLC (San Diego, CA, USA). All other chemicals were sourced from VWR (Radnor, PA, USA) or Sigma-Aldrich (St. Louis, MO).

Synthesis of self-assembling prodrugs (SAPDs). Peptide precursors were synthesized using standard 9-fluorenylmethoxycarbonyl (Fmoc) solid phase peptide synthesis technique. Briefly, Rink Amide MBHA resins were swell in DCM and Fmoc groups were deprotected using a 20% 4-methylpiperidine in DMF solution. The amino acids, for example Fmoc-Lys(Mtt)-OH, were conjugated onto the resins by adding Fmoc-Lys(Mtt)-OH/HBTU/DIEA at a ratio of 4:4:6 (molar equiv to resin) in DMF and the mixture was shaken for 2 h. This Fmoc deprotection and amino acid coupling process was repeated to add more amino acids to the peptide chains. The four peptides have 2, 4, 6, and 8 Fmoc-Lys(Mtt)-OHs, respectively (**Fig. S1**). After that, Mtt groups on the lysine side chain were deprotected by adding 3% TFA/5% TIS/92% DCM for 5 min (repeat 5-6 times), and OEG_5-COOH was subsequently conjugated onto the peptide by amide formation reaction using OEG_5-COOH/ HBTU/DIEA at a ratio of 2:2:3 (molar equiv to resin). After another Fmoc removal, Fmoc-Lys(Fmoc)-OH was added as a branching site for further conjugation of the two Fmoc-Cys(Trt)-OHs. In addition, the the Fmoc groups on the Cysteines were deprotected and acetylated by adding 20% acetic anhydride/DMF solution with 100 μL DIEA. The peptides were cleaved from the resins by adding a mixture of TFA/TIS/H_2O at a ratio of 95:2.5:2.5 and shaking for 3 h. The TFA solution was collected, concentrated, and precipitated in cold diethyl ether. The crude peptides were centrifuged down, washed twice with diethyl ether and dried under vacuum.

The dried peptide solids were purified by HPLC (Varian ProStar Model 325, Agilent Technologies, Santa Clara, CA) with acidic mobile phases (0.1% TFA) of water and acetonitrile. The HPLC was equipped with a Varian Pursuit XRs C18 column (5 μm, 150 × 4.6 mm) for analytical use and a Varian PLRP-S column (100 Å, 10 μm, 150 × 25 mm) for separation purpose. The analytical method was a flow rate of 1 mL/min for 20 mins from 10% acetonitrile to 70% acetonitrile and the preparative method was a flow rate of 20 mL/min for 25 mins from 10% acetonitrile to 40% acetonitrile. The proper fractions were collected and analyzed by ESI-MS using a Finnigan LDQ Deca ion-trap mass spectrometer (Thermo-Finnigan, Waltham, MA) and analytical HPLC again (**Fig. S1** and **S3 – S6**). The final products were concentrated and lyophilized using a FreeZone –105 °C 4.5 L freeze dryer (Labconco, Kansas City, MO).

The purified peptide precursors were further reacted with CPT-etcSS-Pyr prodrug in N_2-purged DMSO over 2 days at the prodrug/peptide ratio of 2.4:1 (1, 2). After the reaction, the separation of the targeted molecules was performed by preparative HPLC again with a flow rate of 20 mL/min for 30 mins from 25% acetonitrile to 65% acetonitrile and monitored at 362 nm. The proper fractions were collected and analyzed by ESI-MS and analytical HPLC (**Fig. S2** and **S7 – S10**). The final products were concentrated and lyophilized using a FreeZone –105 °C 4.5 L freeze dryer (Labconco, Kansas City, MO). Moreover, the lyophilized powders were re-dissolved, calibrated by analytical HPLC, aliquoted into cryo-vials, and re-lyophilized for future use.

Conventional transmission electron microscopy (TEM). SAPDs were dissolved in water at a concentration of 2 mM and aged overnight. The TEM samples were prepared by casting a thin film of sample on a carbon film copper grid (400 square mesh, Electron Microscopy Sciences, Hatfield, PA, USA). 6 μL of sample solution was dropped onto a grid and wicked with a filter paper to create a water film. The sample was negatively stained by uranyl acetate. The grids were dried at room temperature for at least 4 h before TEM imaging (FEI Tecnai 12 TWIN

Transmission Electron Microscope). A SIS Megaview III wide-angle CCD camera was used to acquire the TEM images.

Cryogenic (cryo) TEM. Lacey carbon film supported TEM copper grids (Electron Microscopy Services, Hatfield, PA) were treated with plasma air according to a preset protocol. To make cryo-TEM grids, 6 μL of solution was dropped onto a grid, which was further automatically blotted by filter papers and plunged into a precooled liquid ethane reservoir. The procedures were performed using a Vitrobot and the prepared samples were transferred to a precooled cryo-holder and cryotransfer stage. TEM imaging was performed on the Tecnai 12 microscope with a cryo-holder, and the images were acquired by a 16 bit 2K × 2K FEI Eagle bottom mount camera.

Zeta potential measurement. SAPD solutions at a concentration of 2 mM in PBS buffer (pH = 7.4) were prepared and aged overnight prior to zeta potential measurement. The sample solutions were added in a capillary cell and measured using a Zetasizer Nano ZS90 (Malvern Instruments Ltd., UK). Three repeated measurements for each sample were performed to give the average values and standard deviations.

Circular dichroism (CD) spectroscopy measurement. Stock solutions of four SAPDs were prepared at the concentration of 200 μM and aged overnight before measurement. The sample solutions were loaded into a 1 mm path length quartz UV-Vis absorption cell (Thermo Fisher Scientific, Pittsburgh, PA, USA) and measured from 190 to 480 nm on a Jasco J-710 spectropolarimeter (JASCO, Easton, MD, USA). The obtained spectra were converted from ellipticity (mdeg) to molar ellipticity ($deg \cdot cm^2 \cdot dmol^{-1}$) after subtracting the solvent background.

Cytotoxicity of SAPDs against colon cancer cell lines. Cytotoxicity studies of four SAPDs were investigated on two colon cancer cell lines HT-29 and HCT-116, which were both cultured in DMEM (Invitrogen) containing 10% fetal bovine serum (FBS, Invitrogen) and 1% antibiotics (Invitrogen). HT-29 cell line was a generous gift from Dr. Haiquan Mao lab (MSE, JHU), and HCT-116 cell line was purchased from ATCC. Cancer cells were incubated at 37 °C in a humidified incubator (Oasis, Caron, Marietta, OH, USA) with an atmosphere of 5 % CO_2. The cytotoxicities against two colon cancer cell lines were evaluated using a dose-response study by the SRB method. HT-29 (7000 cells/well) and HCT-116 (5000 cells/well) were seeded into 96-well plates and allowed to attach overnight. Stock solutions of prodrugs at a concentration of 2 mM were prepared and aged overnight, which were then diluted with fresh medium to achieve final CPT concentrations of 0.1, 1, 10, 100, 500, 1000, 5000 and 10000 nM before incubating with cells. Free CPT of same concentrations as above was used as a control, and irinotecan at the concentration of 0.1, 1, 10, 50, 100 and 500 μM was used as another control. The cell viabilities were determined after 72 h incubation using the SRB method according to the manufacturer's protocols (TOX-6, Sigma, St. Louis, MO). The dose-response plots were finally generated by GraphPad Prism 5.

***In vivo* animal studies.** Female athymic nude mice were purchased from the Charles River Laboratories and accommodated at the JHU Animal Care Facility. All the animial procedures were performed under the guidelines approved by the JHU Institutional Animal Care and Use Committee (IACUC). The pharmacokinetics study (Fig. 5 E, F and G) was performed at the Shanghai Institute of Materia Medica, Chinese Academy of Sciences. Female SD rats (200 – 250 g) were purchased from the Shanghai Experimental Animal Center (Shanghai). All animal procedures were performed under guidelines approved by the Institutional Animal Care and Use Committee of the Shanghai Institute of Materia Medica, Chinese Academy of Sciences.

Estimation of SAPD concentration in plasma upon injection. To calculate the concentration after dilution, we simply set the following parameters: body weight of mice (20 g), dosing volume of mice (200 μL), blood volume of mice (1.8 mL), body weight of rat (200 g), dosing volume of mice (1 mL), blood volume of mice (18 mL) and the dosage for both mice and rats (10 mg/kg).

The equation is:

$$\frac{\text{dosage}\,\frac{\text{mg}}{\text{kg}}\ (\text{CPT equivalent}) \times \text{body weight (kg)}}{\text{Mw of CPT} \times 2\ (\text{two CPT on each prodrug}) \times (\text{blood volume} + \text{injected volume})\ \text{mL}} = \text{Concentration upon dilution}$$

In the case of mice, the concentration upon dilution will be:

$$\frac{10\,\frac{\text{mg}}{\text{kg}} \times 0.02\text{kg}}{348.352\,\frac{\text{g}}{\text{mol}}\ (\text{Mw of CPT}) \times 2\ (\text{two CPT on each prodrug}) \times (1.8 + 0.2)\ \text{mL}} = 144\ \mu\text{M}$$

In the case of rats, the concentration upon dilution will be:

$$\frac{10\,\frac{\text{mg}}{\text{kg}} \times 0.2\text{kg}}{348.352\,\frac{\text{g}}{\text{mol}}\ (\text{Mw of CPT}) \times 2\ (\text{two CPT on each prodrug}) \times (18 + 1)\ \text{mL}} = 151\ \mu\text{M}$$

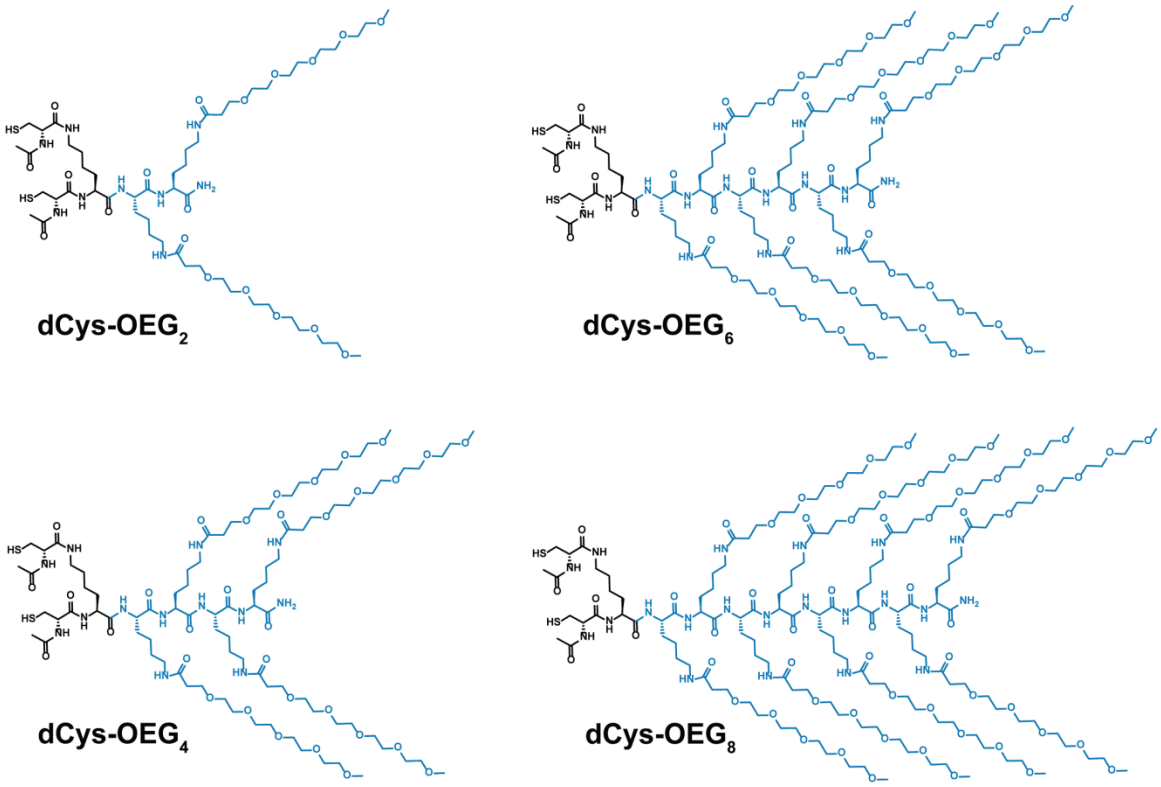

Fig. S1. Chemical structures of the peptide precursors.

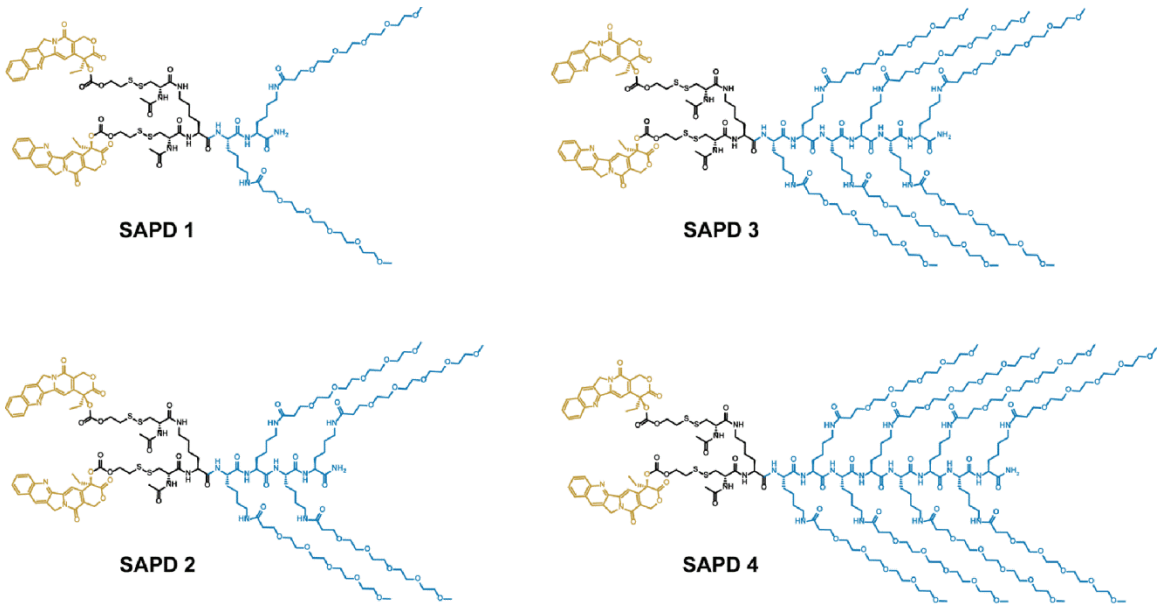

Fig. S2. Chemical structures of the SAPD 1 – 4.

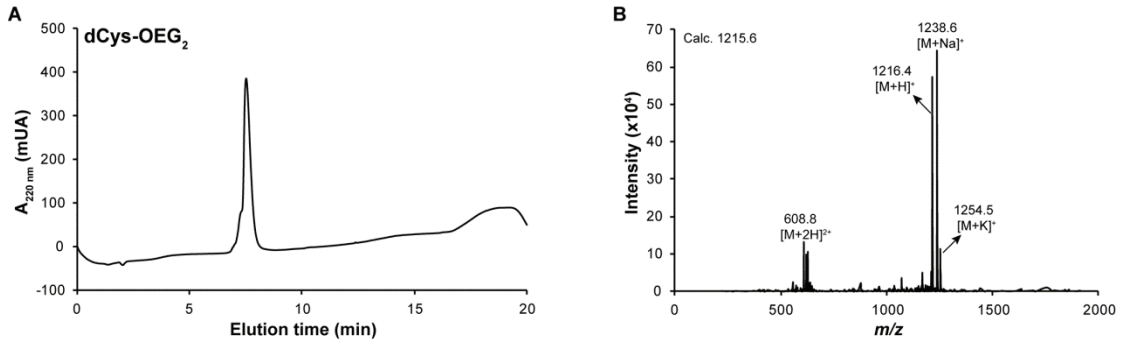

Fig. S3. RP-HPLC (**A**) and ESI-MS (**B**) characterization of dCys-OEG_2. The peaks at 608.8, 1216.4, 1238.8 and 1254.5 correspond to $[M+2H]^{2+}$, $[M+H]^{+}$, $[M+Na]^{+}$ and $[M+K]^{+}$, respectively.

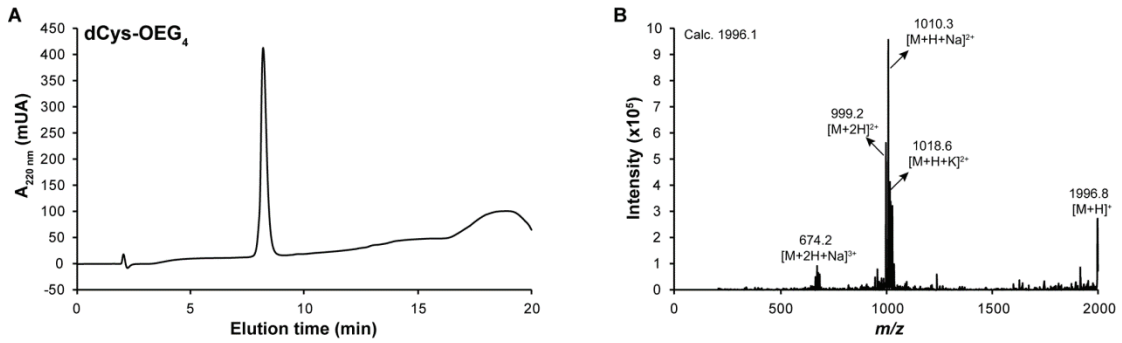

Fig. S4. RP-HPLC (**A**) and ESI-MS (**B**) characterization of dCys-OEG$_4$. The peaks at 674.2, 999.2, 1010.3, 1018.6 and 1996.8 correspond to $[M+2H+Na]^{3+}$, $[M+2H]^{2+}$, $[M+H+Na]^{2+}$, $[M+H+K]^{2+}$ and $[M+H]^{+}$, respectively.

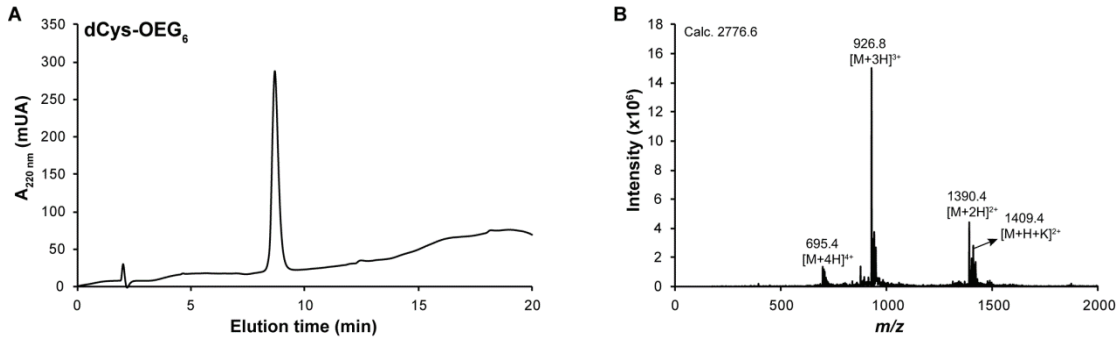

Fig. S5. RP-HPLC (**A**) and ESI-MS (**B**) characterization of dCys-OEG_6. The peaks at 695.4, 926.8, 1390.4 and 1409.4 correspond to $[M+4H]^{4+}$, $[M+3H]^{3+}$, $[M+2H]^{2+}$, and $[M+H+K]^{2+}$, respectively.

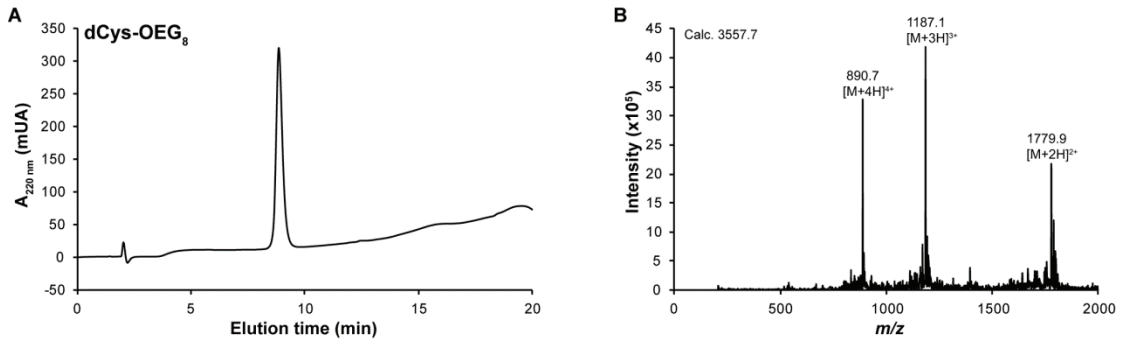

Fig. S6. RP-HPLC (**A**) and ESI-MS (**B**) characterization of dCys-OEG_8. The peaks at 890.7, 1187.1 and 1779.9 correspond to $[M+4H]^{4+}$, $[M+3H]^{3+}$ and $[M+2H]^{2+}$, respectively.

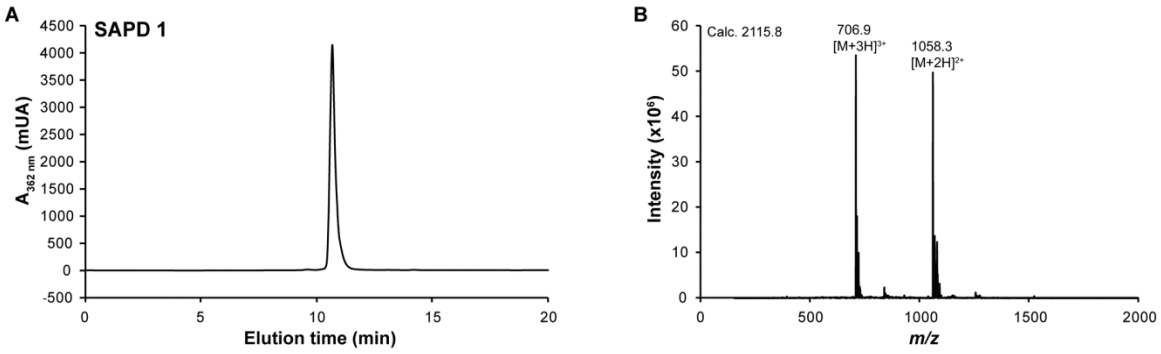

Fig. S7. RP-HPLC (**A**) and ESI-MS (**B**) characterization of SAPD 1. The peaks at 706.9 and 1058.3 correspond to $[M+3H]^{3+}$ and $[M+2H]^{2+}$, respectively.

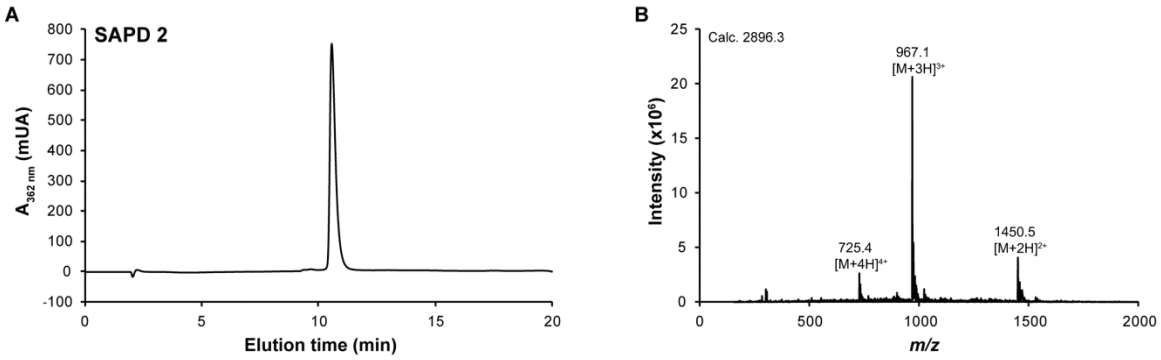

Fig. S8. RP-HPLC (**A**) and ESI-MS (**B**) characterization of SAPD 2. The peaks at 725.4, 967.1 and 1450.5 correspond to $[M+4H]^{4+}$, $[M+3H]^{3+}$ and $[M+2H]^{2+}$, respectively.

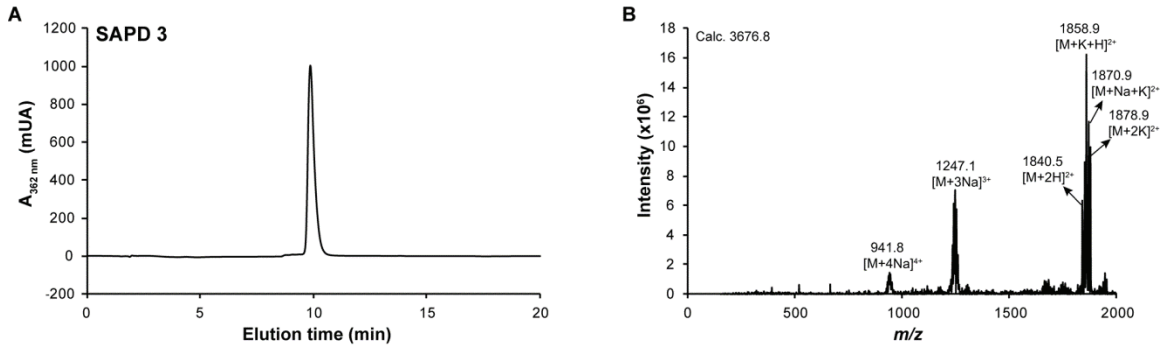

Fig. S9. RP-HPLC (**A**) and ESI-MS (**B**) characterization of SAPD 3. The peaks at 941.8, 1247.1, 1840.5, 1858.9, 1870.9 and 1878.9 correspond to $[M+4Na]^{4+}$, $[M+3Na]^{3+}$, $[M+2H]^{2+}$, $[M+K+H]^{2+}$, $[M+Na+K]^{2+}$ and $[M+2K]^{2+}$, respectively.

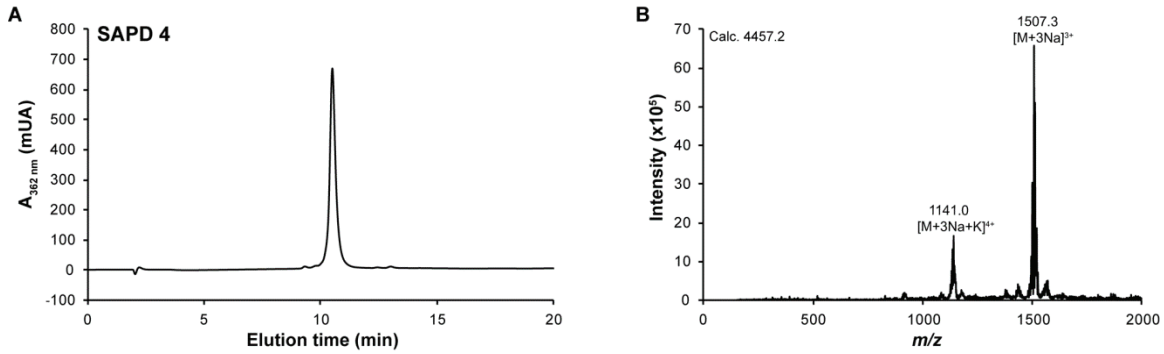

Fig. S10. RP-HPLC (**A**) and ESI-MS (**B**) characterization of SAPD 4. The peaks at 1141.0 and 1507.3 correspond to $[M+3Na+K]^{4+}$ and $[M+3Na]^{3+}$, respectively.

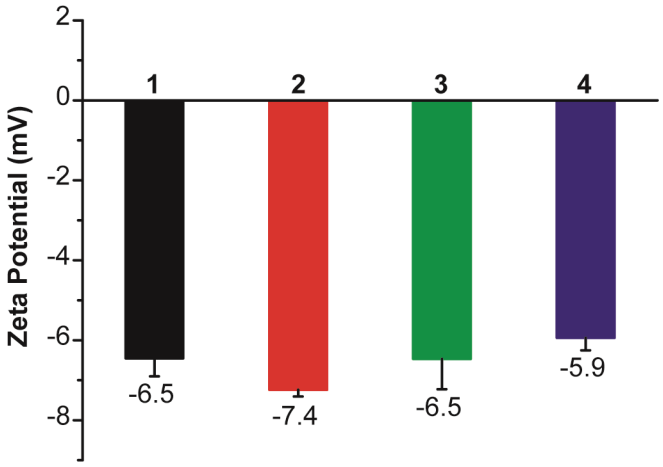

Fig. S11. ζ-Potential values of SAPD 1 – 4 in PBS buffer at pH 7.4 at a concentration of 2 mM. The average values and their standard deviations are calculated from three measurements.

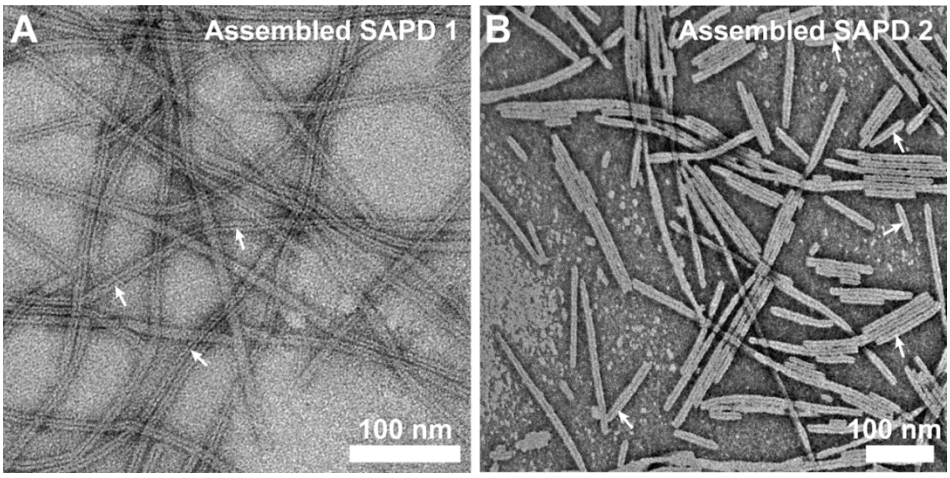

Fig. S12. Conventional TEM images of SAPDs at a concentration of 2 mM in water. SAPD 1 (**A**) and 2 (**B**) self-assembled into filaments with a dark centerline in the middle (pointed out by white arrows). This centerline is a result of deposition of the negative staining agents, indicating a hollowed nature of the filaments, similar to macrocycles. This nanotubular morphology is a result of highly ordered internal packing of CPT moieties in a monolayered fashion.

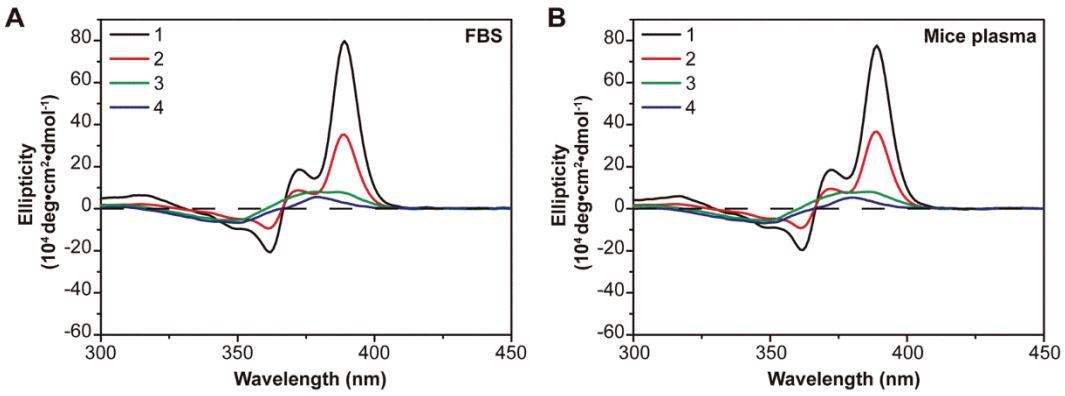

Fig. S13. CD studies in protein environments at 200 μM. CD spectra of SAPDs in 10% FBS (**A**) and 10% mice plasma (**B**). Stock solutions of SAPDs were prepared at 2 mM and aged overnight. The solutions were diluted to 200 μM in 10% fetal bovine serum (FBS), 10% mice plasma and 10% rat plasma (**Fig. 3C**), aged overnight before CD measurement. No obvious changes in the absorptions of SAPD 1 and 2 were observed at the concentration of 200 μM in the protein environments compared with those in aqueous solution (**Fig. 3B**), while slight changes were observed in the cases of SAPD 3 and 4. Thus, we speculate that the serum proteins had negligible effects on stable SAPD 1 and 2 assemblies, but their interactions with monomeric SAPD 3 and 4 can cause some modest changes in their assembly behavior.

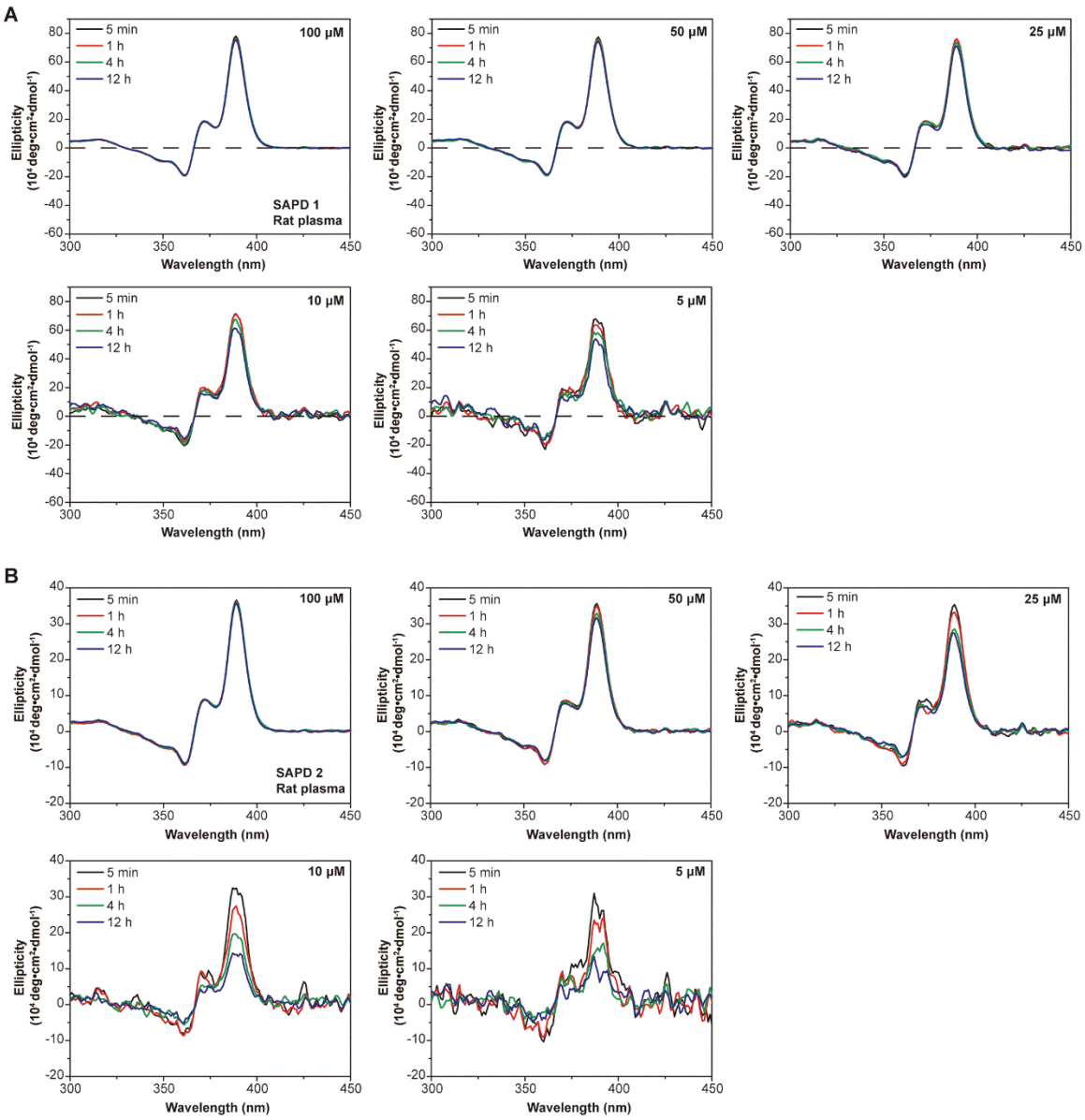

Fig. S14. Kinetic stability of SAPDs in rat plasma upon dilution. Time- and concentration-dependent CD spectra of SAPD 1 (**A**) and SAPD 2 (**B**). The stock solutions (2 mM) of SAPD 1 and 2 were diluted to 100 μM, 50 μM, 25 μM, 10 μM, and 5 μM in 10% rat plasma. The CD spectra were recorded at 5 min, 1h, 4h, and 12 h. SAPD 1 is very stable upon dilution with the final concentration above 25 μM and negligible changes in CD absorption were observed with time. However, dilution of the SAPD 1 to 10 μM and 5 μM resulted in decreased initial CD signals measured at 5 min, and the signals further went down with time, indicating that the dissociation of pre-formed assemblies undergoes a kinetic process. The assemblies tend to disassemble into monomers or oligomers as the concentration approaches the CMC, however, time is needed to fully dissociate or reach the final equilibrium. A similar but pronounced trend was also observed in the case of SAPD 2, which has a higher CMC and its assemblies are considered less stable than SAPD 1 assemblies.

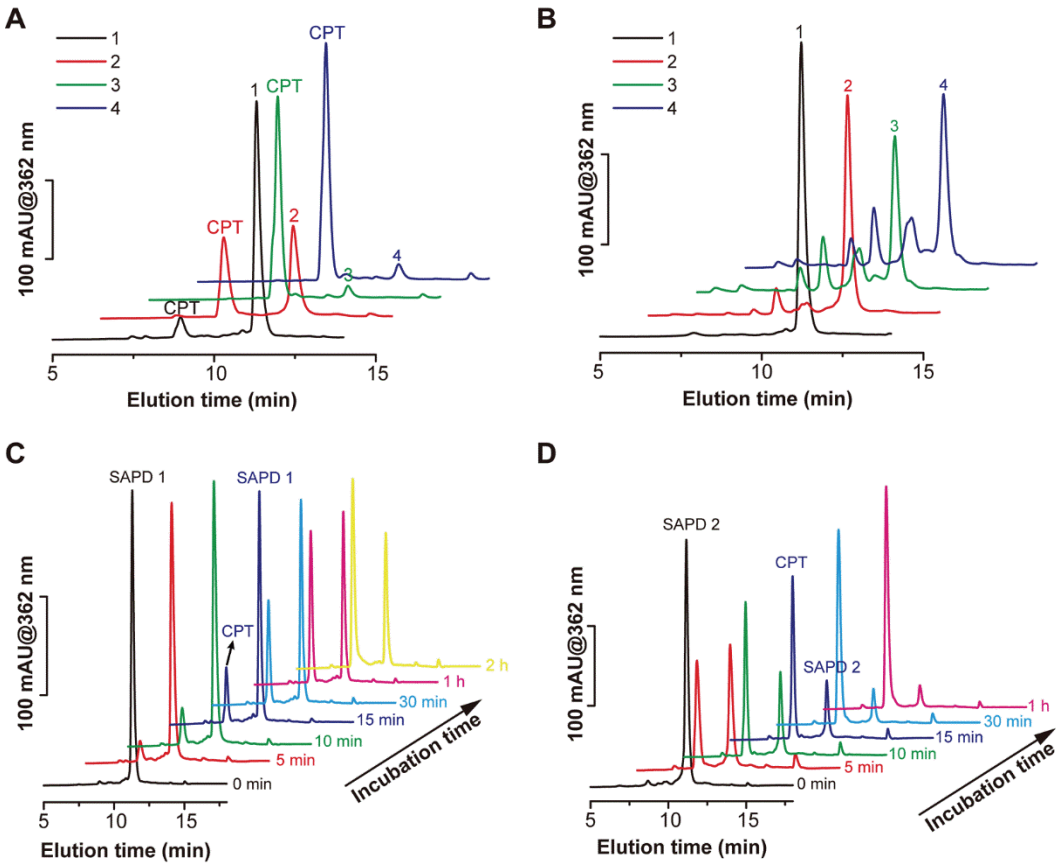

Fig. S15. (**A**) Representative RP-HPLC traces of drug release in GSH environment at 5 min. (**B**) Representative RP-HPLC traces of drug degradation without GSH at 120 h. Representative RP-HPLC traces of drug release of SAPD 1 (**C**) and 2 (**D**) at 200 μM in buffer (PBS, 37℃ and 10 mM GSH). The RP-HPLC traces of SAPD 3 and 4 are not summarized, as more than 90% of the drug released out in 5 minutes.

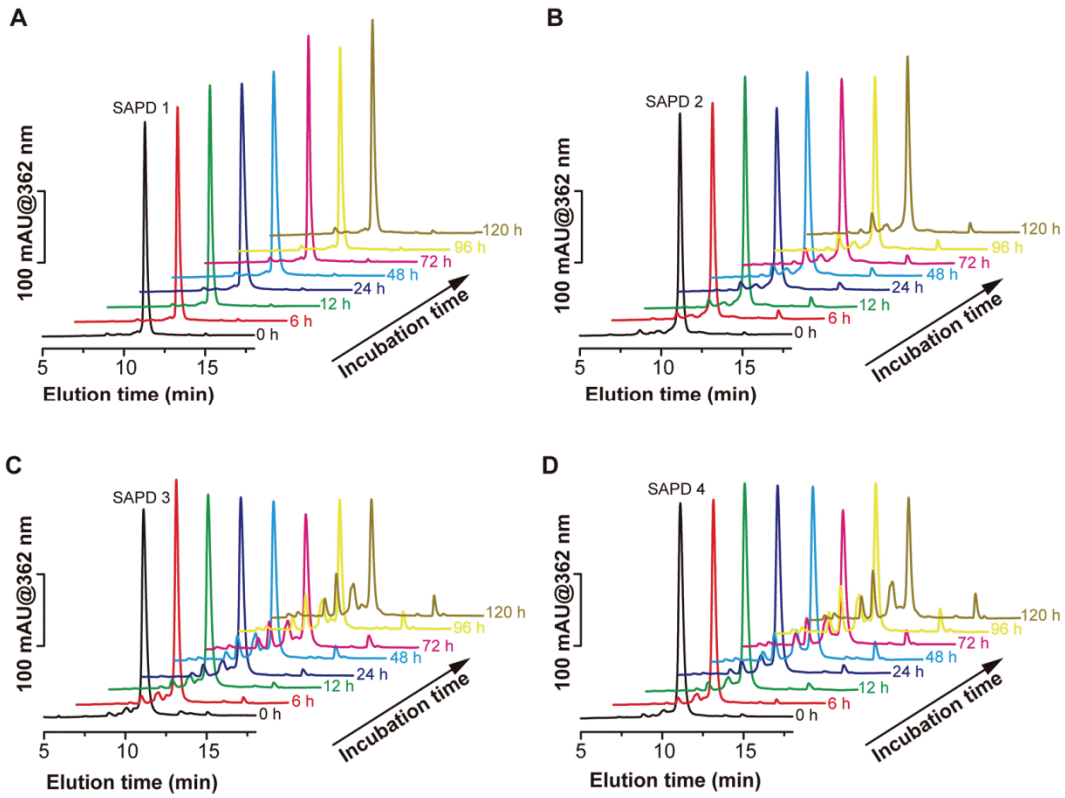

Fig. S16. Representative RP-HPLC traces of degradation of SAPD 1 (**A**), 2 (**B**), 3 (**C**) and 4 (**D**) at 200 μM in PBS at 37℃ without GSH over 120 h.

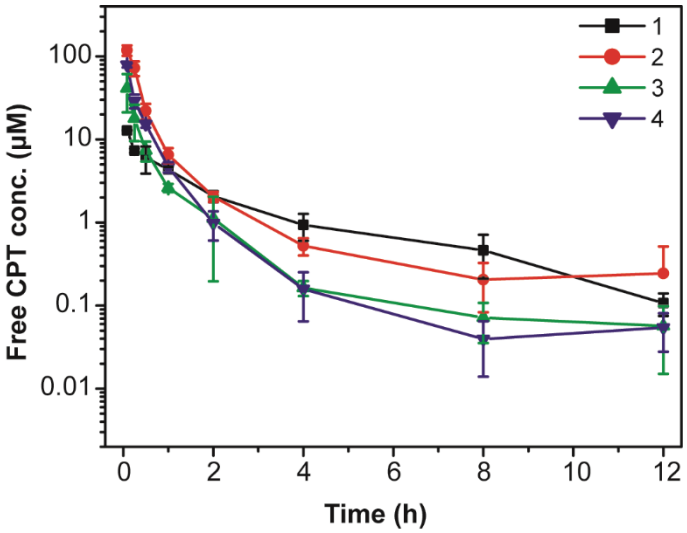

Fig. S17. Concentration of free CPT at various time points in the circulation study of SAPDs. Data represented as n = 3.

Prodrug	Dose (mg/kg)	Maximum %BW loss (day)	Survival/Total
SAPD1	54	20 (3)	0/3
	36	21.2 (3)	0/3
	30	20.6 (4)	1/3
	24	9.8 (3)	3/3
	18	6.5 (1)	3/3
	15	5.0 (2)	3/3
	9	5.1 (1)	3/3
	4.5	0	3/3

Table S1. Summary of maximum tolerated dose (MTD) study of SAPD 1 (3).

References

1. Cheetham AG, Ou YC, Zhang PC, & Cui HG (2014) Linker-determined drug release mechanism of free camptothecin from self-assembling drug amphiphiles. *Chem Commun* 50(45):6039-6042.
2. Cheetham AG, Zhang PC, Lin YA, Lock LL, & Cui HG (2013) Supramolecular Nanostructures Formed by Anticancer Drug Assembly. *J Am Chem Soc* 135(8):2907-2910.
3. Su H, Wang F, Wang Y, Cheetham AG, & Cui HG (2019) Macrocyclization of a Class of Camptothecin Analogues into Tubular Supramolecular Polymers. *J Am Chem Soc* 141(43):17107-17111.